A&A 441, 309–318 (2005)
DOI: 10.1051/0004-6361:20053085

Astronomy & Astrophysics

NLTE ionization equilibrium of Nd II and Nd III in cool A and Ap stars

L. Mashonkina[1,2], T. Ryabchikova[2,3], and A. Ryabtsev[4]

[1] Institut für Astronomie und Astrophysik der UniversitätMünchen, Scheinerstr. 1, 81679 München, Germany
e-mail: lyuda@usm.lmu.de;lima@inasan.ru
[2] Institute of Astronomy, Russian Academy of Science, Pyatnitskaya 48, 119017 Moscow, Russia
[3] Institute for Astronomy, University of Vienna, Türkenschanzstrasse 17, 1180 Vienna, Austria
[4] Institute of Spectroscopy, Russian Academy of Sciences, 142190 Troitsk, Moscow region, Russia

Received 18 March 2005 / Accepted 20 May 2005

Abstract. We investigate the formation of Nd II– III lines in the atmospheres of A-type stars with a comprehensive atomic model including 1651 levels of Nd II, 607 levels of Nd III and the ground state of Nd IV. NLTE leads to overionization of Nd II which weakens the Nd II lines relative to the corresponding LTE line strengths at mild neodymium overabundance ([Nd/H] < 2.5) and amplifies them at higher [Nd/H] values. NLTE abundance corrections grow with the effective temperature and reach 0.6 dex at $T_{\rm eff}$ = 9500 K for [Nd/H] = 2.5. The Nd III lines are strengthened compared with LTE in all cases, and NLTE abundance corrections lie between −0.3 dex and −0.2 dex for $T_{\rm eff}$ between 7500 K and 9500 K. NLTE effects are larger for an inhomogeneous vertical abundance distribution compared with a homogeneous one resulting in positive NLTE abundance correction up to 1.3 dex for the Nd II lines and in negative ones down to −0.5 dex for the Nd III lines. The neodymium distribution in the atmospheres of roAp stars γ Equ and HD 24712 is deduced from NLTE analysis of the Nd II and Nd III lines and a strong evidence is found for the existence of enhanced Nd abundance layers above $\log \tau_{5000} = -3$.

Key words. atomic data – atomic processes – line: formation – line: profiles – stars: atmospheres – stars: chemically peculiar

1. Introduction

Abundance analysis of cool Ap stars revealed for the rapidly oscillating (roAp) stars a huge discrepancy of the order of 1.5–2 dex between neodymium abundances derived from the Nd II and Nd III lines (Ryabchikova et al. 2000, 2001; Gelbmann et al. 2000; Cowley et al. 2000; Kochukhov 2003; Ryabchikova et al. 2004). In further LTE analysis of one of these stars, γ Equ, Ryabchikova et al. (2002) interpreted the observed anomaly as the stratified Nd distribution with the accumulation of the element above $\log \tau_{5000} = -8$. This result is qualitatively consistent with the observed variation of the pulsation radial velocity (RV) amplitude among spectral lines of different elements and their ions. The Nd II and Nd III lines show the maximum RV amplitudes of ∼500–800 m s^{-1}, while the Ba II or Ca I lines of the same intensity have much smaller (<100 m s^{-1}) amplitudes if any. The stratification model proposed by Ryabchikova et al. for γ Equ predicts that Ca, Fe, Ba are concentrated in the deeper atmospheric layers. However, even with the stratified Nd abundances the fits of the line profiles are not good in many cases. In addition, the position of Nd abundance layer above $\log \tau_{5000} = -8$ produces difficulties for an interpretation of the RV pulsation phases derived from the Nd II and Nd III lines and from the core of Hα (see Sachkov et al. 2004a).

In the low density uppermost atmospheric layers a kinetic equilibrium of atoms is expected to deviate from the thermodynamical one. In order to check the earlier conclusions we consider in this work non-local thermodynamical equilibrium (NLTE) line formation for Nd II and Nd III in atmospheres of A-type stars assuming both homogeneous and stratified Nd abundance distribution.

In Sect. 2 we present the method of NLTE calculations for Nd II and Nd III. Theoretical calculations of the Nd II and Nd III atomic structure and transition probabilities and the model atom are described in Sect. 2.1, NLTE effects are considered in Sect. 2.2, and the influence of the uncertainties of stellar atmosphere modeling and atomic parameters on the final results are discussed in Sect. 2.4. In Sect. 3 we obtain the Nd distribution in the atmospheres of two roAp stars γ Equ and HD 24712 from the NLTE analysis of the Nd II and Nd III lines. The obtained results are discussed in Sect. 4 in connection with pulsation properties of the roAp atmospheres.

2. NLTE calculations for Nd II–Nd III

NLTE calculations have been carried out with a revised version of the DETAIL program (Butler & Giddings 1985) using the accelerated lambda iteration following the extremely efficient method described by Rybicki & Hummer (1991, 1992). We use

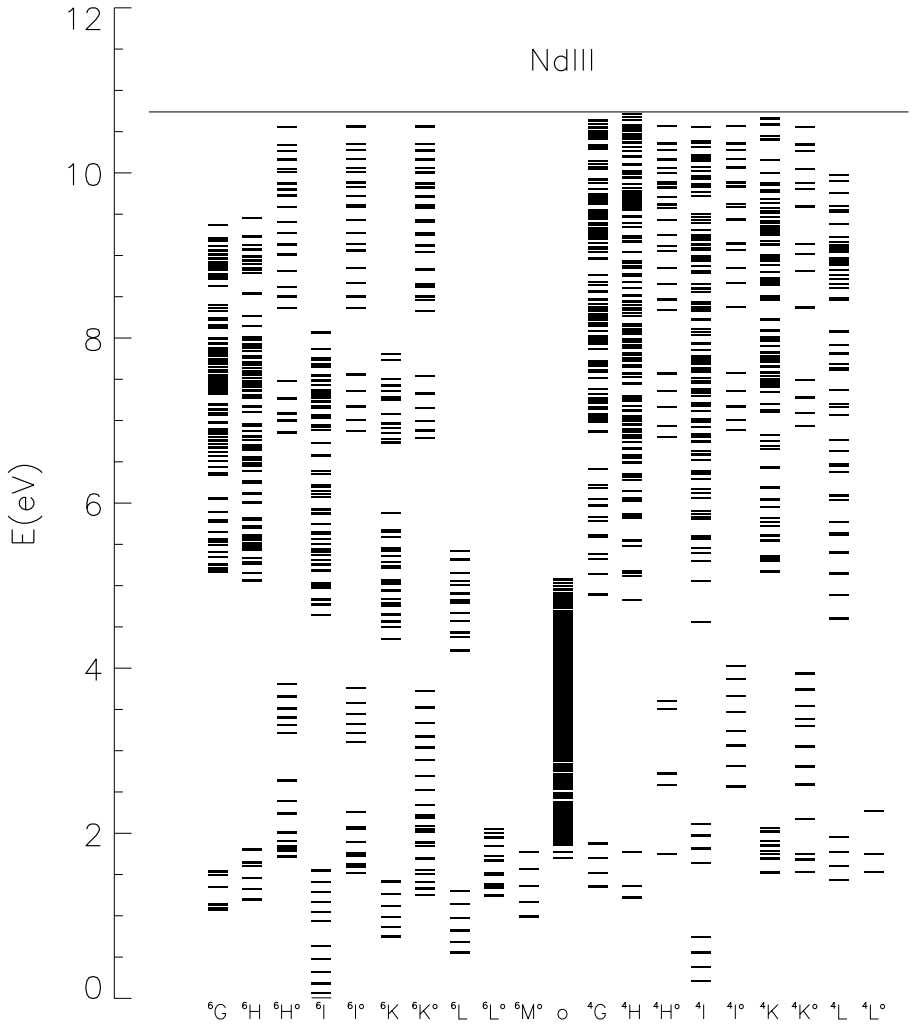

Fig. 1. The Nd II model atom. The measured odd energy levels of unknown terms are shown in the column "o".

homogeneous blanketed model atmospheres computed with the MAFAGS code (Fuhrmann et al. 1997).

2.1. Model atom

The lower levels in singly ionized Nd belong to the $4f^4 6s$ configuration with the $(^5I)^6I$ ground term. Laboratory measurements (Martin et al. 1978; Blaise et al. 1984) give 831 energy levels of Nd II with energy excitation $E_{\rm exc} \le 6$ eV. About a half of them belong to quartet and sextet terms of the $4f^4$ *nl* (*nl* = 6s, 5d, 6p) and $4f^3 5d$ *nl* (*nl* = 5d, 6s) electronic configurations. For most remaining energy levels only the total angular momentum and the parity are known. In line formation layers of the atmospheres with $T_{\rm eff}$ between 7500 K and 8000 K the total number densities of Nd II and Nd III are nearly equal, but Nd II drops rapidly in the hotter atmospheres. To provide the close collisional coupling of Nd II to the continuum electron reservoir we include into a model atom the Nd II high excited levels calculated in this paper for quartet and sextet terms of the $4f^4$ *n*p (*n* = 7–11) and $4f^3 5d$ 6p electronic configurations. The calculations were made using the Cowan code (Cowan 1981). We used "standard" scaling of the Hartree-Fock electrostatic parameters by a factor 0.85. It was found that calculated in this approximation, gf-values for the $4f^4 6s\ ^6I$–$4f^4 6p$ transitions are higher by a factor of 2 to 3 than the accurate laboratory measurements from Den Hartog et al. (2003). A similar accuracy is expected for the predicted gf-values for transitions to the predicted $4f^4 n$p configurations.

Since all investigated Nd II spectral lines arise in transitions between levels with $6 \le L \le 9$, only the terms with $L \ge 4$ are included in a model atom. Radiatively coupled to these terms, the levels of unknown configurations have been added. The latter are shown in Fig. 1 in the column "o". The fine structure is considered for each term. In total, the model atom includes 1651 levels of Nd II (Fig. 1). For the levels taken from Martin et al. (1978) excitation energies have been corrected according to Blaise et al. (1984).

For Nd III the laboratory measurements resulted in 29 energy levels (Martin et al. 1978; Aldenius 2001). Five levels belong to the ground term $4f^4\ ^5I$, and 24 to the triplet and quintet terms of the $4f^3 5d$ excited electronic configuration with $E_{\rm exc} \le$ 5 eV. With such an incomplete term system we cannot get a realistic kinetic equilibrium of Nd III and we use the energy levels calculated in this paper for triplet and quintet terms of the $4f^3 nl$ (*nl* = 4f, 5d, 6s) and $4f^2 5d^2$ electronic configurations. Calculations were made with the Cowan code, as for Nd II.

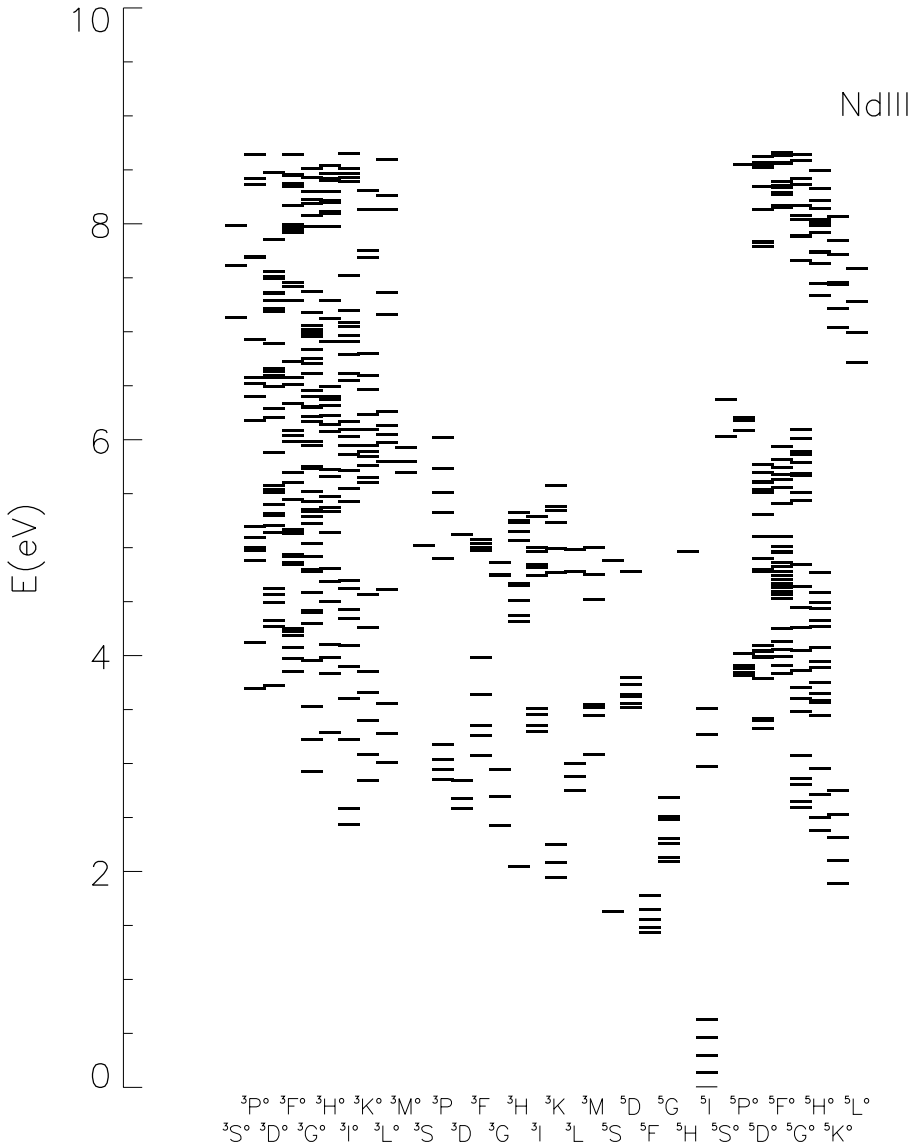

Fig. 2. The Nd III model atom.

Scaling of the Hartree-Fock parameters was made, and the values of the effective interaction parameters were taken according to their trends in the second spectra of lanthanide atoms (Wyart et al. 2005). Our calculated gf-values agree within 20% with the previously published theoretical calculations (Bord 2000; Zang et al. 2002). We include in a model atom all Nd III levels involved in radiative bound–bound ($b - b$) transitions with available laboratory measurements or calculated oscillator strengths, in total, 607 levels of Nd III with $E_{\rm exc} \leq$ 8.66 eV (Fig. 2). In the Nd III case the effect of the highly excited levels missing in the model atom on the kinetic equilibrium is weak because in the atmospheres under investigation departures from LTE in the Nd III level populations are caused mainly by radiative $b - b$ transitions between low-excitation terms.

According to our computations the contribution of the Nd II and Nd III energy levels omitted in the final model atom to the Nd II and Nd III partition functions is 3.5% and 4%, respectively, at $T_{\rm e}$ = 9500 K and even less at lower temperatures. Since Nd II and Nd III together represent a major fraction of the element, such underestimation of partition functions has a negligible effect on level populations and Nd abundances derived from the Nd II and Nd III lines. Levels of the same parity with small energy differences were combined into a single level. The final model atom includes 247 levels of Nd II, 68 levels of Nd III and the ground state of Nd IV.

Oscillator strengths f_{ij} for the transitions between the measured Nd II energy levels were taken from the Vienna Atomic Line Data Base (Kupka et al. 1999) or from recent experimental work by Den Hartog et al. (2003). Oscillator strengths for the transitions from the experimental levels of the $4f^4\ nl$ (nl = 6s, 5d, 6p) electronic configuration to the calculated levels of the $4f^4\ n$p (n = 7–11) and $4f^3$5d 6p electronic configurations and for all transitions between predicted levels have been calculated in this paper. For all Nd III transitions we use f_{ij} computed in this paper, too.

Since no data on the photoionization cross-sections $\sigma_{\rm ph}$ for both the Nd II and Nd III levels are available, we use the hydrogen approximation. We suggest that the photoionization from any Nd II level ends in the ground state of Nd III, $4f^4\,{}^5I_4$. To take into account the photoionization to the remaining levels of the $4f^4\,{}^5I$ term we multiply $\sigma_{\rm ph}$ by the ratio $g(4f^4\,{}^5I)/g(4f^4\,{}^5I_4) \simeq 7$. The photoionization from the $4f^3 5d nl$ levels ends in the excited Nd III $4f^3 5d$ levels, however, we neglect this for two reasons. First, our NLTE calculations show that the most important processes affecting the kinetic equilibrium of Nd II are related to the levels of the $4f^4 6p$ electronic configuration, and second, there is not much sense computing exact threshold wavelengths when approximate photoionization cross-sections are used. The threshold energies of the $4f^3 5d$ *nl* levels are reduced by about 2 eV and, therefore, the photoionization rates are overestimated for the levels with a threshold in the ultraviolet and underestimated for the levels with a threshold in the infrared.

We show below that the kinetic equilibrium of Nd II is mainly controlled by radiative $b-f$ transitions, and the accuracy of photoionization cross-sections is especially important for NLTE calculations. Let us estimate the uncertainty of our approximation. For a certain Nd II level with the principal quantum number of the valence electron $n = 5$ and threshold wavelength $\lambda_{\rm thr} = 1700$ Å the threshold hydrogen cross-section is $\sigma_{\rm thr} = 0.25$ Mb. If n is replaced by the effective principal quantum number $n_{\rm eff} = 2.7$ we obtain $\sigma_{\rm thr} = 5.7$ Mb. Using the Cowan code we have estimated theoretical photoionization cross-sections from the $4f^4(6s+5d)$ levels to the $4f^4\varepsilon p$ continuum. A value of $\sigma_{\rm thr} = 0.2$ Mb was obtained at the threshold consistent with the gf values for the upper $4f^4 np$ (n = 10–12) levels and close to the hydrogen one calculated with principal quantum number n. It is known that the photoionization is essentially a many-body process and should be treated with approximations other than the one used in the Cowan code. Correlations, especially in the final, state would lead to a "giant resonance" in the photoabsorption which would substantially enhance the cross-section. Indeed, laboratory measurements available for some rare-earth neutrals give much higher photoionization cross-sections compared with hydrogen ones. For Eu I $\sigma_{\rm ph}$ exceeds 40 Mb at wavelengths from a threshold for the photoionization at 2186.5 Å to about 2100 Å (Kozlov & Kotochigova 1976). For Yb I $\sigma_{\rm ph}$ is a few Mb at the threshold (1982.5 Å) and there is a broad resonance around 1800 Å with $\sigma_{\rm ph} \simeq 40$ Mb (Kozlov et al. 1976). In our NLTE calculations we use the lowest estimates of photoionization cross-sections based on hydrogen approximation and principal quantum number of levels and, thus, obtain the lower limit for NLTE effects in Nd II.

Electron impact rates for allowed transitions are calculated using the formula of van Regemorter (1962) while Allen's (1973) formula with $\Omega = 1$ is applied to forbidden transitions. Electron impact ionization cross-sections are computed according to Drawin (1961).

We have checked the effect of uncertainties in the input atomic data on the final results. They will be described in Sect. 2.4.

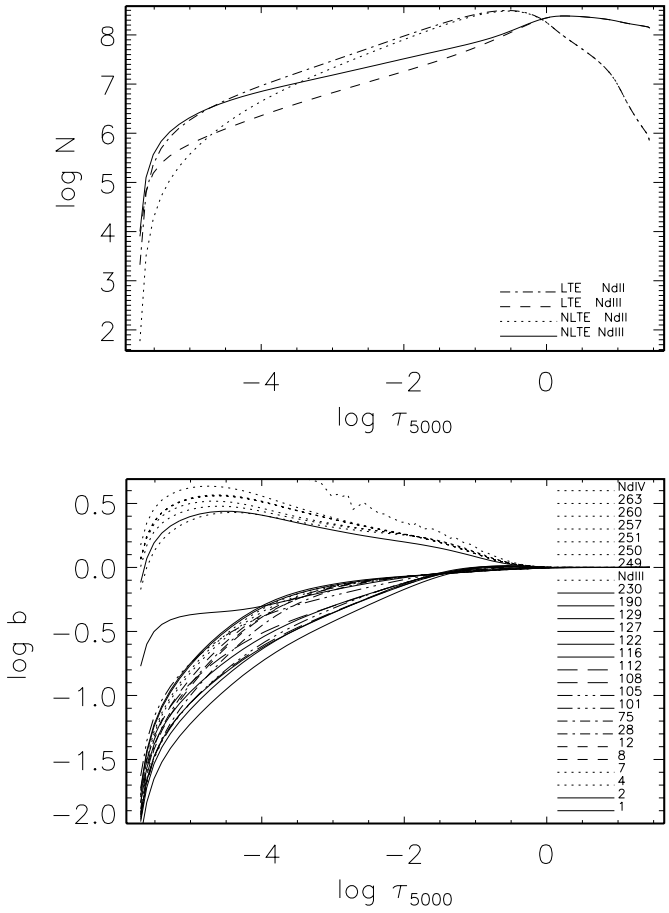

Fig. 3. LTE and NLTE total number densities of Nd II and Nd III (*top panel*) and departure coefficients for selected levels of Nd II and Nd III (*bottom panel*) in the model atmosphere 7700/4.2/0.1. Everywhere in the atmosphere [Nd/H] = 3. The level number corresponds to a successive number of the level in our model atom.

2.2. Kinetic equilibrium calculations and NLTE effects

We demonstrate here that in the atmospheres of dwarfs ($\log g \sim 4$) with $T_{\rm eff}$ between 7500 K and 9500 K the Nd II/Nd III ratio deviates from the thermodynamical value. In the line formation layers all Nd II levels are underpopulated compared with LTE while the Nd III levels are overpopulated at $T_{\rm eff} \le 8000$ K (Fig. 3), while thermodynamical values are preserved at the higher effective temperatures. NLTE effects for the Nd II and Nd III lines have the opposite sign, and they are therefore important for the comparison of Nd abundances derived from these lines. In Fig. 3, bottom panel, the departure coefficients, $b_i = n_i^{\rm NLTE}/n_i^{\rm LTE}$ of the selected levels of Nd II and Nd III in the model atmosphere with $T_{\rm eff}/\log g/$[M/H] = 7700/4.2/0.1 are shown as a function of continuum optical depth τ_{5000} at λ = 5000 Å. This model represents the atmosphere of the roAp star γ Equ (Ryabchikova et al. 2002). Here, $n_i^{\rm NLTE}$ and $n_i^{\rm LTE}$ are the kinetic equilibrium and thermal (Saha-Boltzmann) number densities, respectively. Everywhere in the atmosphere [Nd/H] = 3 is adopted.

The overionization of Nd II in the atmospheric layers above $\log \tau_{5000} = 0$ is caused by a super-thermal radiation of non-local origin near the thresholds of $4f^4 6p$ levels with $E_{\rm exc}$ between

Table 1. List of the investigated Nd II and Nd III lines. Transitions and corresponding level numbers in the model atom are given. The terms with unknown orbital quantum number L are indicated by letter T.

λ [Å]	$E_{\rm low}$ (eV)	Transition	
Nd II			
4706.54	0.00	$4f^4 6s\,^6I_{7/2}$–$4f^3 5d6s\,^6H^\circ_{5/2}$	1–101
4811.34	0.06	$4f^4 6s\,^6I_{9/2}$–unknown $T^\circ_{7/2}$	2–101
6514.96	0.18	$4f^4 6s\,^6I_{11/2}$–$4f^3 5d6s\,T^\circ_{9/2}$	3– 84
4061.08	0.47	$4f^4 6s\,^6I_{15/2}$–$4f^4 6p\,^6K^\circ_{17/2}$	7–122
5533.82	0.56	$4f^4 6s\,^4I_{13/2}$–$4f^3 5d^2\,^4K^\circ_{13/2}$	8–104
5319.82	0.55	$4f^4 5d\,^6L_{11/2}$–$4f^4 6p\,^6K^\circ_{9/2}$	8–105
5165.13	0.68	$4f^4 5d\,^6L_{13/2}$–unknown $T^\circ_{11/2}$	10–110
5077.15	0.82	$4f^4 5d\,^6L_{15/2}$–$4f^3 5d6s\,T^\circ_{13/2}$	12–114
5399.09	0.93	$4f^4 5d\,^6I_{7/2}$–unknown $T^\circ_{5/2}$	14–114
5311.45	0.99	$4f^4 5d\,^6K_{13/2}$–$4f^4 6p\,^6I^\circ_{11/2}$	15–115
5063.72	0.98	$4f^4 5d\,^6L_{17/2}$–unknown $T^\circ_{15/2}$	15–118
5033.51	1.14	$4f^4 5d\,^6L_{19/2}$–unknown $T^\circ_{17/2}$	20–123
6637.19	1.45	$4f^4 5d\,^6H_{9/2}$–$4f^4 6p\,^6I^\circ_{11/2}$	37–115
6680.14	1.69	$4f^4 5d\,^4K_{13/2}$–$4f^4 6p\,^4K^\circ_{13/2}$	51–122
6637.96	1.77	$4f^4 5d\,^4L_{17/2}$–unknown $T^\circ_{15/2}$	58–125
6650.52	1.95	$4f^4 5d\,^4L_{19/2}$–$4f^4 6p\,T^\circ_{17/2}$	75–129
6636.18	2.06	$4f^4 5d\,^4K_{17/2}$–$4f^4 6p\,^4K^\circ_{17/2}$	83–132
Nd III			
5294.10	0.00	$4f^4\,^5I_4$–$4f^3 5d\,^5I^\circ_4$	248–263
6550.23	0.00	$4f^4\,^5I_4$–$4f^3 5d\,^5K^\circ_5$	248–257
4796.49	0.14	$4f^4\,^5I_5$–$4f^3 5d\,^5I^\circ_6$	249–270
5633.55	0.14	$4f^4\,^5I_5$–$4f^3 5d\,^5I^\circ_4$	249–263
6327.26	0.14	$4f^4\,^5I_5$–$4f^3 5d\,^5K^\circ_6$	249–260
6145.07	0.30	$4f^4\,^5I_6$–$4f^3 5d\,^5K^\circ_7$	250–263
6690.83	0.46	$4f^4\,^5I_7$–$4f^3 5d\,^5K^\circ_7$	251–263
5987.68	0.46	$4f^4\,^5I_7$–$4f^3 5d\,^5K^\circ_8$	251–266
5845.02	0.63	$4f^4\,^5I_8$–$4f^3 5d\,^5K^\circ_9$	252–270
5677.18	0.63	$4f^4\,^5I_8$–$4f^3 5d\,^5I^\circ_7$	252–271
5286.75	0.63	$4f^4\,^5I_8$–$4f^3 5d\,^5I^\circ_7$	252–273

3 eV and 4 eV ($\lambda_{\rm thr}$ = 1600–1850 Å). Up to $\log\tau_{5000} \simeq -1.5$ departure coefficients of all the levels with $E_{\rm exc} < 6$ eV are similar due to strong radiative and collisional coupling. The upper layers ($\log\tau_{5000} < -1.5$) become transparent for the radiation of many weak lines arising between low-excitation terms ($E_{\rm exc} <$ 2 eV) and intermediate-excitation terms ($E_{\rm exc}$ = 2.7–4 eV), so the photon loss in these lines increases the underpopulation of the intermediate-excitation terms (level numbers from 105 to 129 in Fig. 3) caused by enhanced photoionization.

A list of investigated Nd II and Nd III spectral lines with the corresponding transitions and level numbers in our model atom is given in Table 1. If the lower or upper level of a transition is involved in a combined level its number density is computed according to its statistical weight. For every investigated Nd II transition $b_i > b_j$ ($i < j$) is obtained, resulting in a source function $S_{ij} \simeq b_j/b_i B_\nu(T_{\rm e}) < B_\nu(T_{\rm e})$ and the amplification of the corresponding spectral line compared with the LTE case. The obtained overpopulation of the Nd III levels leads to the strengthening of the Nd III lines compared with the LTE case. NLTE effects depend on Nd abundance in stellar atmospheres. For the same model atmosphere 7700/4.2/0.1 the Nd II lines are weakened compared with the LTE case if [Nd/H] < 2.5 and intensified for [Nd/H] > 2.5. The Nd III lines are amplified in all cases and NLTE effects grow with increasing [Nd/H]. The theoretical NLTE and LTE equivalent widths of spectral lines together with the NLTE abundance corrections $\Delta_{\rm NLTE} = \log\varepsilon_{\rm NLTE} - \log\varepsilon_{\rm LTE}$ are given in Table 2 (Cols. 4–6) for the model atmosphere 7700/4.2/0.1 representing γ Equ. Oscillator strengths were taken from Den Hartog et al. (2003), if available, or from VALD (Kupka et al. 1999). The mean difference between Den Hartog et al. and VALD data is 0.10 ± 0.08 dex.

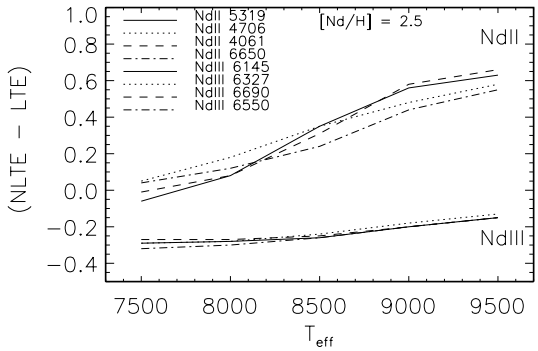

Fig. 4. NLTE abundance corrections for the Nd II and Nd III lines depending on $T_{\rm eff}$. In all cases $\log g$ = 4 and [Nd/H] = 2.5.

As expected, the departures from LTE for the Nd II and Nd III lines grow with $T_{\rm eff}$. The larger $T_{\rm eff}$, the stronger the ultraviolet radiation is, thus resulting in amplifying overionization of Nd II. Assuming [Nd/H] = 2.5 we have calculated $\Delta_{\rm NLTE}$ for several Nd II and Nd III lines for $T_{\rm eff}$ between 7500 K and 9500 K (Fig. 4). NLTE abundance corrections for the Nd II lines are $\Delta_{\rm NLTE} < 0.1$ dex at $T_{\rm eff}$ = 7500 K but they increase with $T_{\rm eff}$ up to ∼0.6 dex at $T_{\rm eff}$ = 9500 K. For the Nd III lines NLTE abundance corrections are negative and nearly independent of $T_{\rm eff}$.

2.3. NLTE effects for stratified Nd abundance distribution

To study the effects of the abundance stratification we performed NLTE calculations for the model atmosphere 7700/4.2/0.1 assuming [Nd/H] = 4 in the atmospheric layers above $\log\tau_{5000} \simeq -3.6$ and a steep decrease of Nd abundance in the deeper layers, so that [Nd/H] = 0 in the layers below $\log\tau_{5000} \simeq -2.7$. The obtained departure coefficients for some levels of Nd II and Nd III are shown in Fig. 5. The theoretical NLTE and LTE equivalent widths together with NLTE abundance corrections are given in Table 2 (columns "layer").

NLTE calculations show the overionization of Nd II and enhanced number density of Nd III in line formation layers similar to the case of a homogeneous Nd abundance distribution. However, in contrast to Fig. 3, we find $b_i < b_j$ for the Nd II levels. The Nd II low-excitation levels are strongly underpopulated above $\log\tau_{5000} = -2$, however, the 105th to 129th levels are even slightly overpopulated between $\log\tau_{5000}$ = 0 and −3.

Table 2. Theoretical NLTE and LTE and observed equivalent widths (in mÅ) of the Nd II and Nd III lines for γ Equ. Computations were made for the model atmosphere 7700/4.2/0.1 for two cases: [Nd/H] = 3 everywhere in atmosphere (columns "[Nd/H] = 3]") and enhanced Nd abundance with [Nd/H] = 4 in atmospheric layers above $\log\tau_{5000} = -3.6$ (columns "layer"). Most of the entries are self-explanatory. The last four columns give the average depth of LTE and NLTE line formation calculated according to Achmad et al. (1991) with the contribution function to the emergent total radiation (column "Line+continuum") and with the contribution function to the emergent line radiation (column "Line").

λ,	$E_{\rm low}$,	$\log gf$	[Nd/H] = 3			layer			$W_{\rm obs}$	$\log\tau_{5000}$			
										Line+continuum		Line	
Å	eV		$W_{\rm LTE}$	$W_{\rm NLTE}$	$\Delta_{\rm NLTE}$	$W_{\rm LTE}$	$W_{\rm NLTE}$	$\Delta_{\rm NLTE}$	mÅ	LTE	NLTE	LTE	NLTE
1	2	3	4	5	6	7	8	9	10	11	12	13	14
Nd II													
4706.54	0.00	−0.71	98	98	0.00	96	48	1.42	40	−4.11	−2.80	−4.95	−4.24
4811.34	0.06	−1.01	86	86	0.00	85	32	1.42	30	−3.74	−1.80	−4.78	−4.09
6514.96	0.18	−1.88	51	48	0.07	52	8	1.13	bl	−1.98	−0.77	−4.34	−3.96
4061.08	0.47	0.55	127	128	−0.03	109	77	1.05	73	−4.32	−3.98	−5.13	−4.60
5533.82	0.56	−1.23	67	67	0.00	63	12	1.39	9	−2.39	−0.98	−4.42	−3.95
5319.82	0.55	−0.14	105	110	−0.12	106	56	1.31	49	−4.30	−3.42	−4.98	−4.25
5165.13	0.68	−0.74	80	83	−0.07	77	28	1.13	bl	−3.35	−1.61	−4.61	−3.98
5077.15	0.82	−1.04	62	62	−0.01	55	12	1.07	7	−1.89	−0.84	−4.36	−3.88
5399.09	0.93	−1.41	44	42	0.03	32	5	0.97	6	−0.88	−0.52	−4.19	−3.85
5311.45	0.99	−0.42	84	87	−0.06	81	32	1.22	31	−3.52	−1.92	−4.64	−4.00
5063.72	0.98	−0.62	73	76	−0.06	68	23	1.04	29	−2.89	−1.26	−4.50	−3.93
5033.51	1.14	−0.47	74	77	−0.07	69	22	1.05	24	−2.88	−1.31	−4.49	−3.91
6637.19	1.45	−0.84	53	54	−0.02	45	7	1.14	19	−1.72	−0.97	−4.25	−3.88
6680.14	1.69	−0.72	50	52	−0.04	40	5	1.15	bl	−1.51	−0.93	−4.21	−3.85
6637.96	1.77	−0.32	68	72	−0.06	61	17	1.00	32	−2.35	−1.29	−4.32	−3.89
6650.52	1.95	−0.11	66	71	−0.09	63	16	1.10	25	−2.54	−1.43	−4.34	−3.90
6636.18	2.06	−0.94	26	25	0.02	15	1	1.07	bl	−0.73	−0.58	−4.09	−3.84
Nd III													
5294.10	0.00	−0.70	105	124	−0.42	106	127	−0.51	143	−4.38	−4.67	−5.13	−5.16
6550.23	0.00	−1.50	77	99	−0.40	86	112	−0.48	120	−3.68	−4.42	−4.78	−4.94
4796.49	0.14	−1.66	57	69	−0.27	53	70	−0.37	83	−1.64	−3.73	−4.48	−4.62
5633.55	0.14	−2.19	34	48	−0.26	31	55	−0.43	67	−0.92	−2.63	−4.32	−4.33
6327.26	0.14	−1.42	74	94	−0.37	81	104	−0.42	123	−3.50	−4.37	−4.73	−4.90
6145.07	0.30	−1.34	74	94	−0.36	78	99	−0.40	131	−3.19	−4.27	−4.67	−4.83
6690.83	0.46	−2.36	20	32	−0.27	17	38	−0.46	53	−0.74	−1.84	−4.24	−4.18
5987.68	0.46	−1.27	67	87	−0.37	70	91	−0.38	108	−2.94	−4.28	−4.60	−4.81
5845.02	0.63	−1.18	63	82	−0.35	64	82	−0.33	110	−2.63	−4.22	−4.54	−4.75
5677.18	0.63	−1.43	54	68	−0.26	49	64	−0.27	90	−1.61	−3.85	−4.40	−4.60
5286.75	0.63	−1.79	34	45	−0.22	27	40	−0.30	56	−0.72	−2.84	−4.27	−4.35

For each investigated Nd II transition we find that $S_{ij} > B_\nu(T_{\rm e})$ and $b_i < 1$ in line formation layers, so the corresponding spectral line is weakened compared to the LTE case, thus resulting in the large NLTE abundance corrections of 1.00 dex to 1.42 dex for different lines. The strong amplification of NLTE effects for the Nd II lines compared with the case of homogeneous Nd abundance distribution is caused by the shift of the line formation layer upward where the departure coefficients of different levels deviate significantly from 1 and from each other. The Nd III lines are strengthened compared with the LTE case, approximately at the same level as for the homogeneous Nd abundance distribution.

2.4. Uncertainties in stellar atmosphere modeling and atomic parameters

Stellar atmosphere modeling. Ryabchikova et al. (2002) presented evidence for the abundance gradients in the atmosphere of γ Equ. They find that Ca, Cr, Fe, Ba, Si and Na are overabundant in deeper atmospheric layers and normal to underabundant in the upper layers with an abundance jump in the region of $-1.5 < \log\tau_{5000} < -0.5$. The excess or depletion of the elements as a function of depth will modify the atmospheric structure. The effect should be particularly important when a stratification of iron group elements takes place.

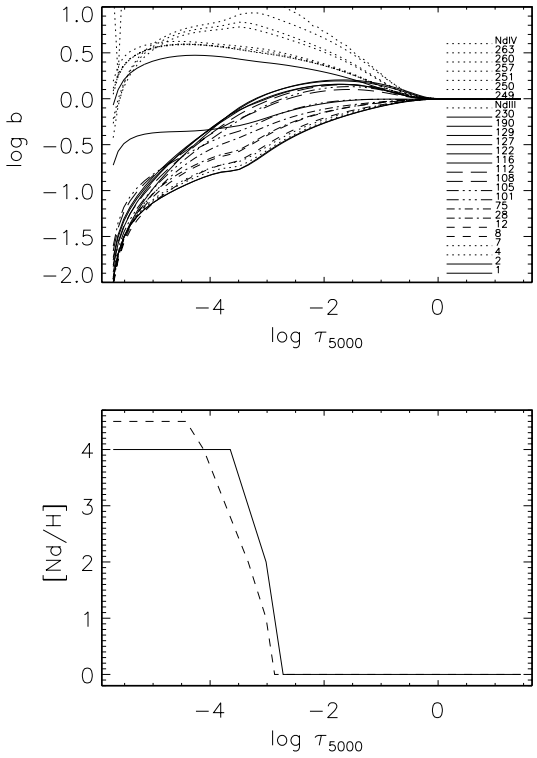

Fig. 5. Departure coefficients ($\log b$) for selected levels of Nd II (with the level numbers between 1 and 230) and Nd III (up to the level number 263) in the model atmosphere 7700/4.2/0.1 with the [Nd/H] ratio distribution shown in bottom panel by solid line. Dashed line in the bottom panel shows the obtained [Nd/H] ratio distribution in the atmosphere of HD 24712.

For γ Equ [Fe/H] = −2.5 at $\log\tau_{5000} < -1$ and [Fe/H] = +1 in the deeper layers; [Cr/H] $\simeq -1$ at $\log\tau_{5000} < -0.6$ and [Cr/H] = +1.6 in the deeper layers. A similar abundance stratification is found for 53 Cam (Babel 1992; Babel & Lanz 1992) and β CrB (Wade et al. 2001). LeBlanc & Monin (2004) constructed self-consistent model atmospheres where abundance gradients caused by radiative diffusion are calculated in each iteration. The diffusion models predict the correct position of the abundance jumps, but too low abundances in the uppermost atmospheric layers compared with the empirical distributions. For the atmospheric parameters representing γ Equ we have calculated the model atmosphere using the empirical abundance gradients found by Ryabchikova et al. (2002) and LLMODELS atmospheric code which provides the accurate line absorption treatment in opacity calculations (Shulyak et al. 2004). The difference in temperature between homogeneous and stratified model atmospheres is negligible in the outer atmosphere at $\log\tau_{5000} < -2$. The temperature in the stratified atmosphere is higher by 3–4% at depths larger than $\tau_{5000} = 1$ and lower by up to 200 K in the layers between $\log\tau_{5000} = -0.5$ and −2 compared to the homogeneous model atmosphere. It is important that the fluxes computed from both model atmospheres are similar over a wide spectral range from the visible to the UV. Thus, including the empirically derived stratification for a few elements in model calculations does not affect the results of our NLTE calculations for Nd II–Nd III.

Atomic parameters. First, we test the photoionization cross-sections for the Nd II levels, because the kinetic equilibrium of Nd II depends strongly on radiative $b-f$ transitions. Since the departures from LTE in the Nd II lines are especially important for the inhomogeneous Nd abundance distribution we perform NLTE calculations for this case using various photoionization cross-sections for the Nd II levels. When the hydrogenous photoionization cross-sections are increased by a factor of 100 the overionization of Nd II is amplified and $\Delta_{\rm NLTE}$ increases by 0.09 dex to 0.14 dex for different Nd II lines. For the Nd III lines NLTE effects are slightly strengthened, too; namely, by 0.02 dex in terms of NLTE abundance correction. Reducing the hydrogen photoionization cross-sections by a factor of 100 has much larger effect on both the Nd II and Nd III lines: the absolute value of $\Delta_{\rm NLTE}$ decreases by 0.36 dex to 0.65 dex for different Nd II lines and by 0.10 dex to 0.14 dex for the Nd III lines. We emphasize that even with lowest photoionization cross-sections the ionization equilibrium Nd II/Nd III deviates significantly from the thermodynamical one; for example, for γ Equ the difference of Nd abundances derived from the Nd II and Nd III lines drops by about 1 dex compared to that found from the LTE analysis. Thus, only in the case when the hydrogen approximation significantly overestimates photoionization cross-sections for the Nd II levels would it affect the position of the enhanced Nd abundance layer; namely, the layer will be shifted outward. However, as was discussed above, the adopted approximation gives the lower limit for the photoionization cross-sections, so we under- rather than overestimate NLTE effects in our NLTE calculations. We believe that an uncertainty of photoionization cross-sections does not change our conclusion as regards the existence of a inhomogeneous distribution of Nd in the atmospheres of the investigated stars.

It can be expected that varying cross-sections of the electron impact excitation has a stronger effect on the Nd III kinetic equilibrium compared with Nd II, because, contrary to Nd II, NLTE effects for Nd III are mainly due to $b-b$ transitions. An influence of the uncertainty of collisional cross-sections should be larger for the homogeneous Nd abundance distribution because in this case even at [Nd/H] = 3 the Nd III lines form in the deeper layers compared with the stratified Nd abundance distribution. For example, in the model atmosphere with $T_{\rm eff}$ = 7700 K and $\log g = 4.2$ the Nd III λ6145 line core forms around $\log\tau_{5000} \simeq -3.5$ for the homogeneous Nd abundance distribution with [Nd/H] = 3 and around $\log\tau_{5000} \simeq -5.2$ for the stratified Nd abundance distribution. The corresponding values are $\log\tau_{5000} \simeq -0.7$ and −2.5 for the Nd III λ6690. As expected, an increase in collision excitation cross-sections by a factor of 10 leads to weakening NLTE effects: for the homogeneous Nd abundance distribution NLTE abundance corrections are smaller by 0.02 dex to 0.05 dex for the Nd II lines and by 0.1 dex in absolute value for the Nd III lines. Thus, the uncertainty of collisional rates does not affect our further analysis of neodymium distribution in the atmospheres of the investigated stars.

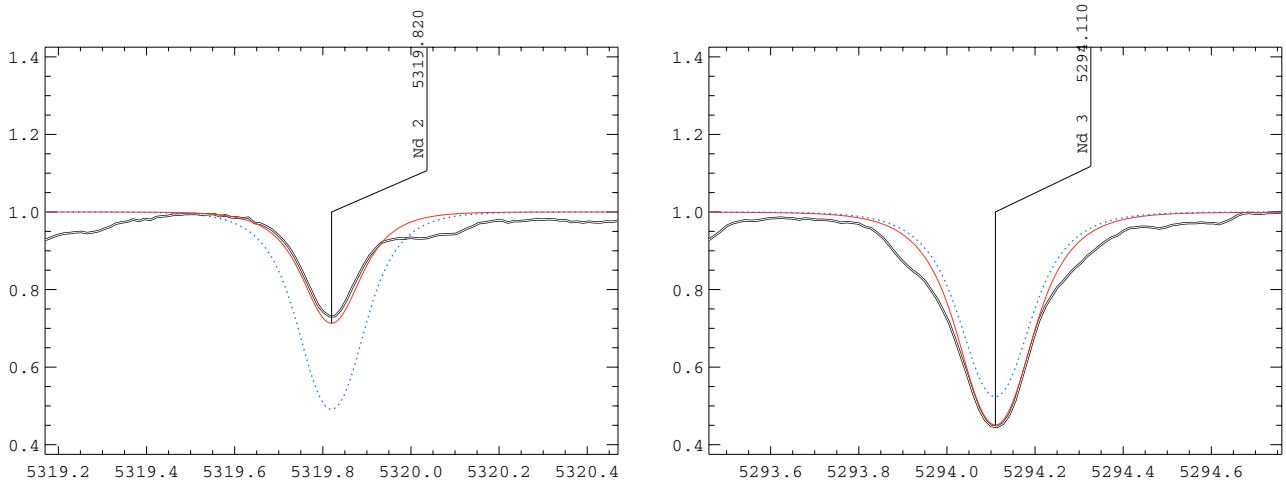

Fig. 6. Theoretical NLTE (solid line) and LTE (dotted line) Nd II λ5319 (*left panel*) and Nd III λ5294 (*right panel*) line profiles calculated with the stratified Nd abundance distribution shown in Fig. 5 compared with the observed spectrum (double line) of γ Equ.

3. Nd abundance distribution in the atmospheres of roAp stars γ Equ and HD 24712

Our calculations show that at the assumption of homogeneous Nd abundance distribution in the atmospheres with $T_{\rm eff} \leq$ 8200 K (typical for roAp stars) NLTE effects may explain only 0.5 dex of the difference between LTE abundances derived from the Nd II and Nd III lines and not the 1.5–2.0 dex observed in roAp stars (see Ryabchikova et al. 2001). NLTE calculations have been performed for the stratified Nd abundance distribution. Based on them we analyse the Nd II and Nd III lines in the two roAp stars γ Equ and HD 24712.

γ Equ. The results of LTE and NLTE calculations for γ Equ are presented in Table 2. Equivalent widths in γ Equ (the tenth column in Table 2) were measured using the spectra described by Sachkov et al. (2004a) and Kochukhov et al. (2004). Figure 6 shows a comparison between the observed and synthetic NLTE and LTE line profiles for the two Nd II and Nd III lines. The adopted Nd abundance distribution is shown in Fig. 5 (bottom panel). The influence of the magnetic field on line intensity in γ Equ was simulated by a microturbulence value of 1.5 km s^{-1} (Ryabchikova et al. 1997a). Owing to the adopted assumptions and possible errors in the model atmosphere parameters for γ Equ we do not attempt to reach an exact coincidence between the observed and computed equivalent widths, so our stratification model may be considered as first approximation. However, it provides a much better agreement between observations and calculations than the LTE stratification model derived by Ryabchikova et al. (2002). The position of the Nd abundance jump is shifted down from $\log \tau_{5000} = -8$ in the LTE model to -3.2 in the NLTE model. We note that the NLTE value is close to the depth formation of the Hα core which extends from $\log \tau_{5000} = -2$ to -5 in the LTE approximation. A study of the Balmer lines based on NLTE line formation is in progress and the results will be presented in a forthcoming paper. For the stratified Nd distribution we have calculated the LTE and NLTE average optical depths of line formation as a center-of-gravity in wavelength domain using intensity of the line points as weights. We follow Achmad et al. (1991) with taking (i) the contribution function to the emergent total (continuum + line) radiation (Table 2, Cols. 11, 12); and (ii) the contribution function to the emergent line radiation (Table 2, Cols. 13, 14). It was emphasized by Achmad et al. (1991) that the second approach provides a more realistic depth of line formation, in particular for weak lines, for which the continuum contribution shifts the average depth formation downward. This effect becomes much more important for the case of a stratified atmosphere. When the contribution function to the total (continuum + line) radiation is used the line formation depth of most Nd II lines is shifted well below the enhanced Nd abundance layer.

HD 24712. Ryabchikova et al. (2001) derived a +1.46 dex difference between LTE Nd III and Nd II abundances (we call it the Nd III/Nd II ionization anomaly). NLTE effects in a homogeneous atmosphere may explain a maximal difference of +0.2 to +0.3 dex. Again, it is impossible to achieve Nd III/Nd II ionization equilibrium without introducing an enhanced Nd abundance layer in the upper atmosphere. LTE and NLTE calculations of the Nd III and Nd II lines were performed for the model atmosphere with $T_{\rm eff}$ = 7250 K and $\log g$ = 4.3 which represents the atmosphere of HD 24712 (Ryabchikova et al. 1997b). Equivalent widths in HD 24712 (Table 3) were measured using the spectra taken at the maximum of the magnetic field and of the REE line intensity (Sachkov et al. 2004b). Magnetic intensification in HD 24712 was again mimicked by a microturbulence value of 1 km s^{-1} (Ryabchikova et al. 1997b). Table 3 contains the results of LTE and NLTE calculations for the Nd abundance distribution in the atmosphere of HD 24712 shown in Fig. 5 by the dashed line.

Tables 2, 3 and Fig. 6 demonstrate a fairly good agreement between observations and calculations, providing strong evidence for a Nd concentration above $\log \tau_{5000} = -3$. The newly found Nd abundance distribution is more realistic that derived by Ryabchikova et al. (2002) with the LTE assumption.

Table 3. Theoretical NLTE and LTE (columns "layer") and observed equivalent widths (in mÅ) of the Nd II and Nd III lines in HD 24712. Computations were made for the model atmosphere 7250/4.3/–0.1 with the stratified Nd abundance distribution shown in Fig. 5. The average depths of LTE and NLTE line formation calculated with the contribution function to the emergent line radiation (Achmad et al. 1991) are given in the two last columns.

λ,	layer			$W_{\rm obs}$	$\log \tau_{5000}$	
Å	$W_{\rm LTE}$	$W_{\rm NLTE}$	$\Delta_{\rm NLTE}$	mÅ	LTE	NLTE
Nd II						
6514.96	64	17	1.39	15	−5.02	−4.61
5319.82	95	60	1.15	62	−5.34	−5.03
5165.13	73	38	1.10	45	−5.20	−4.70
5077.15	59	22	1.09	26	−5.04	−4.54
5311.45	75	41	1.16	40	−5.21	−4.75
5063.72	66	33	1.05	36	−5.14	−4.63
6680.14	50	13	1.16	23	−4.85	−4.47
Nd II						
5294.10	84	112	−0.77	108	−5.38	−5.42
6327.26	69	95	−0.66	109	−5.22	−5.32
6145.07	66	89	−0.62	106	−5.17	−5.28
6690.83	17	38	−0.46	53	−4.81	−4.80
5987.68	59	82	−0.59	96	−5.12	−5.28
5845.02	54	75	−0.53	93	−5.07	−5.26
5677.18	43	62	−0.48	88	−4.96	−5.18
5286.75	24	43	−0.51	53	−4.84	−4.99

4. Discussion

Using a full NLTE analysis we have failed to remove the disparity between Nd abundances derived from the Nd II and Nd III lines under the assumption of a homogeneous Nd abundance distribution in the atmospheres of two roAp stars. We found, however, that introducing a layer with a strongly enhanced Nd abundance in the outer atmosphere provides a natural way to describe the Nd II and Nd III lines for the unique distribution of the Nd. The required Nd overabundance in the layer is [Nd/H] = 4 at $\log \tau_{5000} < -3.5$ for γ Equ and [Nd/H] = 4.5 at $\log \tau_{5000} < -4.5$ for HD 24712. We expect that the Hα core and the Nd II and the weakest Nd III lines should form in the same atmospheric layers, given the similarity of their pulsation RV amplitudes and, in particular, phases (Sachkov et al. 2004a). Indeed, the present NLTE analysis suggests that the Nd II and Nd III lines form closer to the layers where the cores of hydrogen lines probably form.

From our study we conclude that any analysis of pulsation properties of the roAp atmospheres based on the Nd lines has to be performed using the NLTE approach. NLTE effects may be particularly important for the stars where the Nd II and Nd III lines show different pulsation behavior. For example, in the roAp star 33 Lib (HD 137949) the pulsation radial velocities of some Nd II lines vary approximately in anti-phase with the RVs of the Nd III lines (Mkrtichian et al. 2003). Moreover, the pulsation pattern of the Nd II 5319.82 Å line in this star is different from that for Nd III 6145.07 Å: the first line shows pulsations at two frequencies, 2.015 and 4.030 mHz, with nearly equal amplitudes, while the RV pulsations of the Nd III line occur mainly at the first frequency (Kurtz et al. 2004). The star 33 Lib ($T_{\rm eff}$ = 7550 K, $\log g$ = 4.3) has even a larger Nd III/Nd II ionization anomaly (of ~2.0 dex) than γ Equ and HD 24712 (Ryabchikova et al. 2004). Therefore, we expect neodymium stratification in the atmosphere of 33 Lib, too. Both Mkrtichian et al. (2003) and Kurtz et al. (2004) suggest the existence of a pulsation node in the atmosphere of 33 Lib with Nd II and Nd III line formation on both sides of this node. However, if the neodymium stratification in 33 Lib has the same structure as obtained in the present paper for the two roAp stars, then the overlapping of the line formation layers for some Nd II (4061, 4706, 5319) and Nd III (5286, 6691, 5291) lines will take place (see the last columns in Tables 2, 3); we predict a similar pulsation behavior (frequency pattern, pulsation phases and amplitudes) of these lines. Rare-earth element stratification analysis in roAp stars based on NLTE line formation will provide extremely important information about the distribution of the pulsations through the stellar atmosphere.

Acknowledgements. The authors thank Prof. Thomas Gehren for providing the code MAFAGS. All NLTE calculations were performed using computer equipment of the Institute of Astronomy and Astrophysics, Ludwig-Maximilians University Munich. L.M. and T.R. acknowledge the Presidium RAS Program "Non-stationary phenomena in astronomy", RFBR grant number 04-02-16788 and the Federal Program "Astronomy", and the Austrian Science Fond FwF, project P17-580-N02 (TR) for partial financial support.

References

Achmad, I., de Jager, C., & Nieuwenhuijzen, H. 1991, A&A, 250, 445
Aldenius, M. 2001, Master Thesis, Department of Physics, Univ. of Lund
Allen, C. W. 1973, Astrophysical Quantities (Athlone Press)
Babel, J. 1992, A&A, 258, 449
Babel, J., & Lanz, T. 1992, A&A, 263, 232
Blaise, J., Wyart, J.-F., Djerad, M. T., & Ahmed, Z. B. 1984, Phys. Scr., 29, 119
Bord, D. J. 2000, A&AS, 144, 517
Butler, K., & Giddings, J. 1985, Newsletter on the analysis of astronomical spectra, No. 9, University of London
Cowan, R. D. 1981, The Theory of Atomic Structure and Spectra (Berkeley, California, USA: Univ. of California Press)
Cowley, C. R., Ryabchikova, T., Kupka, F., et al. 2000, MNRAS, 317, 299
Den Hartog, E. A., Lawler, J. E., Sneden, C., & Cowan, J. J. 2003, ApJS, 148, 543
Drawin, H.-W. 1961, Z. Phys., 164, 513
Fuhrmann, K., Pfeiffer, M., Frank, C., Reetz, J., & Gehren, T. 1997, A&A, 323, 909
Gelbmann, M., Ryabchikova, T. A., Weiss, W. W., et al. 2000, A&A, 356, 200
Kochukhov, O. 2003, A&A, 404, 669
Kochukhov, O., Ryabchikova, T., & Piskunov, N. 2004, A&A, 415, L13
Kozlov, M. G., & Kotochigova, S. A. 1976, Optika i Spectroscopiya, 41, 360
Kozlov, M. G., Kotochigova, S. A., & Nikolaev, V. N. 1976, Optika i Spectroscopiya, 41, 10

Kupka, F., Piskunov, N., Ryabchikova, T. A., Stempels, H. C., & Weiss, W. W. 1999, A&AS, 138, 119
Kurtz, D. W., Elkin, V. G., Mathys, G., et al. 2004, The A-Star Puzzle, IAUS 224, ed. J. Zverko, W. W. Weiss, J. Žižňovský, & S. J. Adelman, 343
LeBlanc, F., & Monin, D. 2004, The A-Star Puzzle, IAUS 224, ed. J. Zverko, W. W. Weiss, J. Žižňovský, & S. J. Adelman, 193
Martin, W. C., Zalubas, R., & Hagan, L. 1978, Atomic energy levels – The Rare Earth Elements, NSRDS-NBS 60 (Washington: US Gov. Print. Off.)
Mkrtichian, D. E., Hatzes, A. P., & Kanaan, A. 2003, MNRAS, 345, 2003
Ryabchikova, T. A., Adelman, S. J., Weiss, W. W., & Kuschnig, R. 1997a, A&A, 322, 234
Ryabchikova, T. A., Landstreet, J. D., Gelbmann, M. J., et al. 1997b, A&A, 327, 1137
Ryabchikova, T. A., Savanov, I. S., Hatzes, A. P., Weiss, W. W., & Handler, G. 2000, A&A, 357, 981
Ryabchikova, T. A., Savanov, I. S., Malanushenko, V. P., & Kudryavtsev, D. O. 2001, Astron. Rep., 45, 382
Ryabchikova, T., Piskunov, N., Kochukhov, O., et al. 2002, A&A, 384, 545
Ryabchikova, T., Nesvacil, N., Weiss, W. W., Kochukhov, O., & Stütz, C. 2004, A&A, 423, 705
Rybicki, G. B., & Hummer, D. G. 1991, A&A, 245, 171
Rybicki, G. B., & Hummer, D. G. 1992, A&A, 262, 209
Sachkov, M., Ryabchikova, T., Kochukhov, O., et al. 2004a, Variable Stars in the Local Group, IAU Coll., 193, ed. D. W. Kurtz, & K. Pollard, ASP Conf. Ser., 310, 208
Sachkov, M., Ryabchikova, T., Ilyin, I., Kochukhov, O., & Lüftinger, T. 2004b, The A-Star Puzzle, IAUS 224, ed. J. Zverko, W. W. Weiss, J. Žižňovský, & S. J. Adelman, on-line (http://uk.cambridge.org/journals/journal_new_2005.asp#IAU), 770
Shulyak, D., Tsymbal, V., Ryabchikova, T., Stütz, Ch, & Weiss, W. W. 2004, A&A, 428, 993
van Regemorter, H. 1962, ApJ, 136, 906
Wade, G. A., Ryabchikova, T. A., Bagnulo, S., & Piskunov, N. 2001, in Magnetic fields across the Hertzsprung-Russel diagram, ed. G. Mathys, S. K. Solanki, & T. Wickramasinghe, ASP Conf. Ser., 248, 341
Wyart, J.-F., Tchang-Brillet, W.-Ü. L., Churilov, S. S., & Ryabtsev, A. N. 2005, Phys. Scr., in press
Zang, Z. G., Svanberg, S., Palmery, P., Quinet, P., & Biémont, E. 2002, A&A, 385, 724